

# Doubly and Triply Linked Porphyrin–Perylene Monoimides as Near IR Dyes with Large Dipole Moments and High Photostability

Chongjun Jiao,<sup>†</sup> Kuo-Wei Huang,<sup>‡</sup> Chunyan Chi,<sup>†</sup> and  
Jishan Wu<sup>\*,†</sup>

<sup>†</sup>Department of Chemistry, National University of Singapore, 3 Science Drive 3, 117543, Singapore, and <sup>‡</sup>KAUST Catalysis Center and Division of Chemical and Life Sciences and Engineering, 4700 King Abdulaziz University of Science and Technology, Thuwal 23955-6900, Kingdom of Saudi Arabia

*chmwuj@nus.edu.sg*

Received September 27, 2010

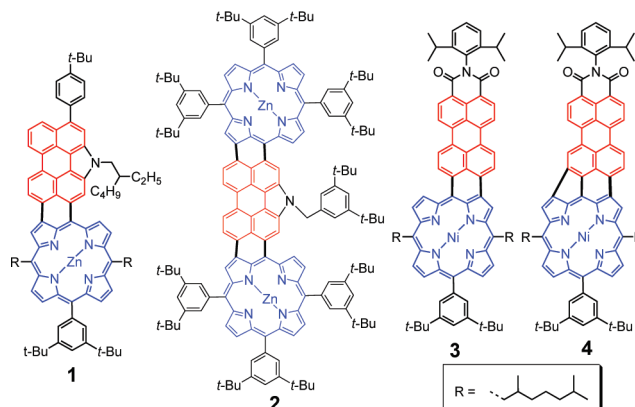
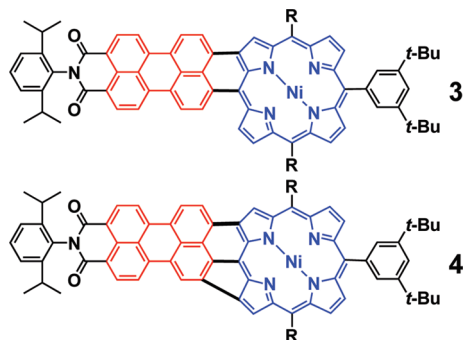


**FIGURE 1.** Structures of perylene-fused porphyrins **1–4**.



Doubly and triply linked porphyrin–perylene monoimides **3** and **4**, with extraordinary stability, large dipole moments, and strong near IR absorption, were prepared by means of one-pot oxidative cyclodehydrogenation promoted by FeCl<sub>3</sub>.

Near Infrared (NIR) dyes<sup>1</sup> are defined as compounds that function (absorption and/or emission) in the spectral region ranging from 700 to 2000 nm. Recently, studies on NIR dyes have sparked considerable interest owing to their diverse applications, such as organic photovoltaics,<sup>2</sup> nonlinear optics,<sup>3</sup> and bioimaging.<sup>4</sup> How to obtain stable NIR dyes, however, remains a challenge. The fusion of aromatic rings to porphyrin

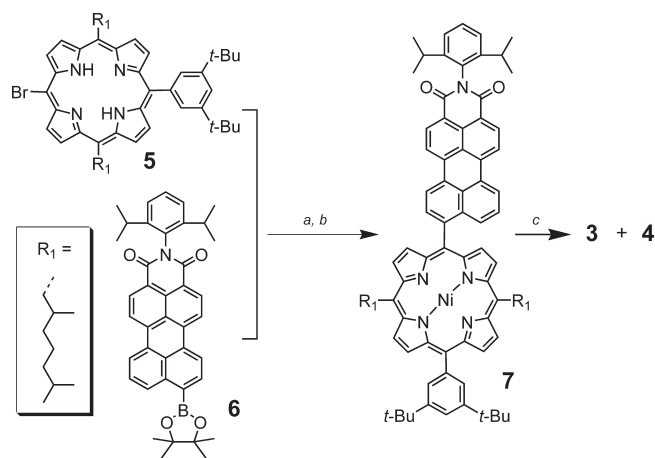
cores<sup>5</sup> has received much attention because these hybrid molecules with  $\pi$ -extended cores and low symmetries inevitably exhibit unusual optical and electronic properties including NIR absorption, making them attractive for numerous applications, such as NIR photodetectors,<sup>6</sup> photovoltaics,<sup>5h</sup> semiconductors,<sup>7</sup> and two-photon absorption materials.<sup>5c</sup>

A general strategy used to obtain aromatic ring-fused porphyrins is the intramolecular ring-closure reaction of the singly linked porphyrin–aromatic ring dyads, which normally can be prepared by Pd-promoted cross-coupling reactions between appropriate derivatives of aromatic compounds and porphyrin building blocks<sup>5f,g,i</sup> or by direct cross-condensation of dipyrromethanes and the aldehydes.<sup>5c</sup> Our group recently reported the syntheses of *N*-annulated perylene-fused porphyrins (**1** and **2** in Figure 1) with enhanced NIR absorption and emission.<sup>8</sup> Although **1** and **2** are stable upon exposure to visible light, their solutions gradually decompose upon UV irradiation. The moderate stability of **1** and **2** can be attributed to the high electron density in these highly conjugated systems, making them slowly oxidize by singlet oxygen in the air upon irradiation with UV light. In our previous work,<sup>9</sup> we have found that the electron-withdrawing

- (1) (a) Fabian, J.; Nakanazumi, H.; Matsuoka, M. *Chem. Rev.* **1992**, *92*, 1197–1226. (b) Qian, G.; Wang, Z. *Chem. Asian J.* **2010**, *5*, 1006–1029.
- (2) (a) Li, C.; Liu, M.; Pschirer, N. G.; Baumgarten, M.; Müllen, K. *Chem. Rev.* **2010**, *110*, 6817–6855. (b) Wang, X. -Z.; Wong, W. -Y.; Cheung, K. -Y.; Fung, M. -K.; Djurisić, A. B.; Chan, W. -K. *Dalton Trans.* **2008**, 5484–5494. (c) Wang, X. -Z.; Ho, C. -L.; Yan, L.; Chen, X.; Chen, X.; Cheung, K. -Y.; Wong, W. -Y. *J. Inorg. Organomet. Polym.* **2010**, *20*, 478–487.
- (3) (a) Kim, H. M.; Cho, B. R. *Chem. Commun.* **2009**, 153–164. (b) Pawlicki, M.; Collins, H. A.; Denning, R. G.; Anderson, H. L. *Angew. Chem., Int. Ed.* **2009**, *48*, 3244–3266.
- (4) (a) Kiyose, K.; Kojima, H.; Nagano, T. *Chem. Asian J.* **2008**, *3*, 506–515. (b) Amiot, C. L.; Xu, S. P.; Liang, S.; Pan, L. Y.; Zhao, X. J. *Sensors* **2008**, *8*, 3082–3105.

- (5) (a) Lash, T. D.; Werner, T. M.; Thompson, M. L.; Manley, J. M. *J. Org. Chem.* **2001**, *66*, 3152–3159. (b) Richeter, S.; Jeandon, C.; Kyritsakas, N.; Ruppert, R.; Callot, H. J. *J. Org. Chem.* **2003**, *68*, 9200–9208. (c) Gill, H. S.; Marmjan, M.; Santamaria, J.; Finger, I.; Scott, M. J. *Angew. Chem. Int. Ed.* **2004**, *43*, 485–490. (d) Yamane, O.; Sugiyara, K.; Miyasaka, H.; Nakamura, K.; Fujimoto, T.; Nakamura, K.; Kaneda, T.; Sakata, Y.; Yamashita, M. *Chem. Lett.* **2004**, *33*, 40–41. (e) Kurotobi, K.; Kim, K. S.; Noh, S. B.; Kim, D.; Osuka, A. *Angew. Chem., Int. Ed.* **2006**, *45*, 3944–3947. (f) Tanaka, M.; Hayashi, S.; Eu, S.; Umeiyama, T.; Matano, Y.; Imahori, H. *Chem. Commun.* **2007**, 2069–2071. (g) Davis, N. K. S.; Pawlicki, M.; Anderson, H. L. *Org. Lett.* **2008**, *10*, 3945–3947. (h) Tokuji, S.; Takahashi, Y.; Shinmori, H.; Shinokubo, H.; Osuka, A. *Chem. Commun.* **2009**, 1028–1030. (i) Davis, N. K. S.; Thompson, A. L.; Anderson, H. L. *Org. Lett.* **2010**, *12*, 2124–2127. (j) Diev, V. V.; Hanson, K.; Zimmerman, J. D.; Forrest, S. R.; Thompson, M. E. *Angew. Chem., Int. Ed.* **2010**, *49*, 5523–5526.
- (6) Zimmerman, J. D.; Diev, V. V.; Hanson, K.; Lunt, R. R.; Yu, E. K.; Thompson, M. E.; Forrest, S. R. *Adv. Mater.* **2010**, *22*, 2780–2783.
- (7) Sayyad, M. H.; Saleem, M.; Karimov, K. S.; Yaseen, M.; Ali, M.; Cheong, K. Y.; Noor, A. F. M. *Appl. Phys. A: Mater. Sci. Process.* **2009**, *98*, 103–109.
- (8) Jiao, C.; Huang, K.-W.; Guan, Z.; Xu, Q.-H.; Wu, J. *Org. Lett.* **2010**, *12*, 4046–4049.
- (9) Jiao, C.; Huang, K.-W.; Luo, J.; Zhang, K.; Chi, C.; Wu, J. *Org. Lett.* **2009**, *11*, 4508–4511.

## SCHEME 1. Synthetic Route toward Compounds 3 and 4



(a)  $\text{Pd}(\text{PPh}_3)_4$ ,  $\text{Cs}_2\text{CO}_3$ , toluene/DMF; (b)  $\text{Ni}(\text{acac})_2$ , toluene; 59% for two steps; (c)  $\text{FeCl}_3$ , nitromethane, DCM, 38% for 3 and 25% for 4.

dicarboxylic imide groups can significantly lower the high-lying HOMO energy level of the respective *N*-annulated perylene and quaterylene, which are unstable upon long-term exposure to air and light. Perylene monoimide, possessing a strong electron-withdrawing imide group, was thus considered to be a rational building block to replace the relatively electron-rich *N*-annulated perylene unit in the perylene-fused porphyrin compounds. Herein, we present an unprecedented one-pot synthesis of doubly and triply linked porphyrin–peryene monoimides **3** and **4** (Figure 1), which are expected to possess improved stability compared to the electron-rich dyes **1** and **2**. In the meanwhile, a “push–pull” structure is constructed in **3** and **4** that can result in further red-shift of the absorption spectra. More importantly, such a push–pull structure can facilitate a fast electron injection from the excited dye to the conduction band of  $\text{TiO}_2$  in dye-sensitized solar cells,<sup>2</sup> thus qualifying **3** and **4** as promising light-harvesting NIR dyes after replacement of the 2,6-diisopropylphenyl groups with an anchoring group.<sup>10</sup> The connection between the perylene and porphyrin unit can also be modified by chemistry, with doubly *peri-meso*; *peri-β* linkage in **3** and triply *peri-β*; *peri-meso*; *meta-β'* linkage in **4**, and this difference should also result in tunable optical and electronic properties. Given the electron-withdrawing character of carboximide and the difficulty in fusing the inactive aromatic compound to the porphyrin core, a new cyclization method will have to be developed.

As shown in Scheme 1, porphyrin monobromide **5**<sup>8</sup> was chosen as the key intermediate with the aim of enhancing the solubility of the target molecules. Precursor **7** was synthesized by Suzuki coupling of **5** with **6**<sup>11</sup> followed by metalation. Ring closure of **7** using  $\text{Sc}(\text{OTf})_3/\text{DDQ}$  herein could not afford the cyclized compound of the perylene monoimide fused porphyrin

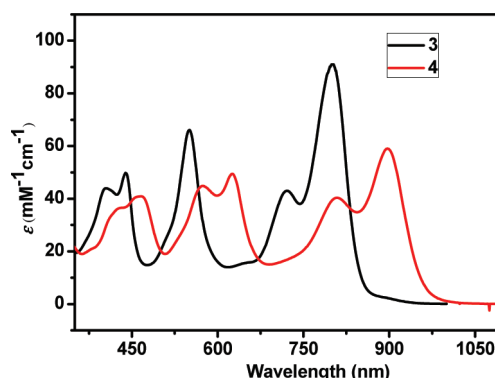


FIGURE 2. UV–vis–NIR absorption spectra of **3** and **4** in toluene ( $1.0 \times 10^{-5}$  M).

because of the presence of an electron-deficient carboximide group; thus other conditions for the cyclodehydrogenation had to be used. Iron(III) chloride is known as a mild oxidant for the cyclodehydrogenation of many branched oligophenylenes into polycyclic aromatic hydrocarbons.<sup>12</sup> Recently, this reagent has been successfully applied for the preparation of naphthyl-fused porphyrin carboxylic acid.<sup>5f</sup> Since the Zn-porphyrin usually undergoes demetalation reaction upon treatment with a strong Lewis acid including  $\text{FeCl}_3$ , herein Ni-containing porphyrin precursor **7** was used. Cyclization of **7** with 10-fold excess  $\text{FeCl}_3$  at reflux conditions in anhydrous dichloromethane (DCM) generated doubly linked porphyrin–peryene monoimide **3** in 38% yield, which had a purple color. To our surprise, an unanticipated green compound was also isolated in 25% yield, which has been proven to be the triply linked porphyrin–peryene monoimide **4**, as confirmed by MALDI-TOF mass spectrometry and 1D and 2D  $^1\text{H}$  NMR characterization (see Supporting Information). To the best of our knowledge, this is the first example to demonstrate that not only the *peri*-positions but also the *meta*-position of perylene monoimide can be involved in the cyclodehydrogenation to form a highly  $\pi$ -conjugated system. Such an unusual multiple C–C bond formation could account for the high reactivity of the Ni-porphyrin at the  $\beta$ -positions<sup>13</sup> and the refluxing reaction conditions. Moreover, no cyclized product was obtained when the reaction was carried out at room temperature.

Compounds **3** and **4** have good solubility in common organic solvents. As shown in Figure 2, both **3** and **4** show broad absorption spectra that cover the entire visible and a part of the NIR spectral regions. The absorption maximum of **3** was found at 803 nm, while a further red-shift of 94 nm was observed for **4** compared with **3**, owing to the higher conjugation in **4**. Noteworthy is that perylene monoimide-fused porphyrins **3** and **4** exhibit remarkably intense NIR absorption, with molar extinction coefficients  $\epsilon = 91\,000$  and  $59\,000\text{ M}^{-1}\text{ cm}^{-1}$  at long-wavelength maximum, respectively. Compound **3**, in particular, displays the strongest Q bands among aromatic ring-fused monoporphyrim hybrid molecules.<sup>5</sup> Unlike *N*-annulated perylene-fused porphyrins **1** and **2**, compounds **3** and **4**, possessing electron-deficient perylene monoimide as well as electron-donating porphyrin,

(10) (a) Edvinsson, T.; Li, C.; Pschirer, N.; Schöneboom, J.; Eickemeyer, F.; Sens, R.; Boschloo, G.; Herrmann, A.; Müllen, K.; Hagfeldt, A. *J. Phys. Chem. C* **2007**, *111*, 15137–15140. (b) Li, C.; Yum, J.-H.; Moon, S.-J.; Herrmann, A.; Eickemeyer, F.; Pschirer, N. G.; Erk, P.; Schöneboom, J.; Müllen, K.; Grätzel, M.; Nazeeruddin, M. K. *ChemSusChem* **2008**, *1*, 615–618. (c) Li, C.; Liu, Z.; Schöneboom, J.; Eickemeyer, F.; Pschirer, N. G.; Erk, P.; Herrmann, A.; Müllen, K. *J. Mater. Chem.* **2009**, *19*, 5405–5415.

(11) Weil, T.; Reuther, E.; Beer, C.; Müllen, K. *Chem.—Eur. J.* **2004**, *10*, 1398–1414.

(12) Wu, J.; Pisula, W.; Müllen, K. *Chem. Rev.* **2007**, *107*, 718–747.

(13) Tsuda, A.; Furuta, H.; Osuka, A. *J. Am. Chem. Soc.* **2001**, *123*, 10304–10321.

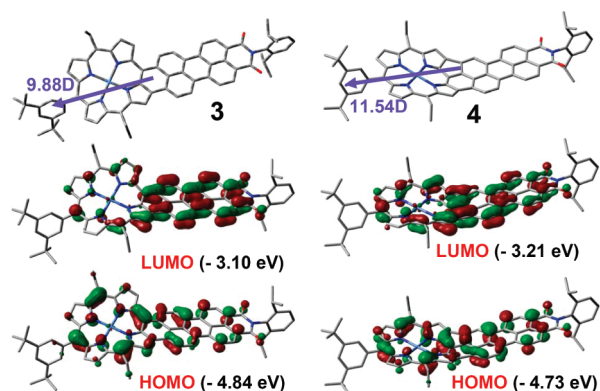


**FIGURE 3.** Optimized molecular structures, dipole moments (indicated by arrows), and frontier molecular orbital profiles of molecules **3** and **4** (the branched aliphatic chains are replaced by ethyl during the TD-DFT calculations).

exhibit only very weak fluorescence,<sup>14</sup> presumably due to the intramolecular charge transfer as well as the presence of Ni<sup>2+</sup> ion, both of which quench fluorescence.

Time-dependent density function theory (TDDFT at B3LYP/6-31G\*\*) calculations were conducted for **3** and **4** to further understand their geometric and electronic structures. Their optimized molecular structures, dipole moments, and the frontier molecular orbital profiles are shown in Figure 3. The perylene moiety in **3** slightly deviates from the porphyrin plane due to the steric hindrance between the  $\beta$ -proton of porphyrin and the *meta*-proton of the perylene core, while the entire molecule **4** turns out to be bowl shaped due to the fusion of the five-membered ring. The HOMO is predominantly localized on the porphyrin core, while the LUMO is mainly localized on the perylene monoimide unit for both **3** and **4**, and this asymmetry obviously gives rise to different dipole moments, which are calculated as 9.88 and 11.54 D, respectively. Such orbital partitioning and large dipole moments are beneficial to sensitizers for dye-sensitized solar cells.<sup>2a</sup> TDDFT calculations also predict that each compound exhibits three major absorption bands, and the longest absorption maxima for **3** and **4** are located at 756.9 and 976.7 nm. These data agree well with our experimental results (Figure 2).

Cyclic voltammetry was employed to investigate the redox behavior of **3** and **4** (Figure 4 and Table S1). Compound **3** in dry DCM exhibits two reversible oxidation waves with half-wave potentials ( $E_{\text{ox}}^n$ ) at 0.37 and 0.77 V (vs Fc<sup>+</sup>/Fc), while three reversible oxidative waves were observed with  $E_{\text{ox}}^n$  at 0.20, 0.43, and 0.77 V for **4**. It is obvious that the triply linked compound **4** has a larger extended pi-system, which can stabilize the multiple charges. Furthermore, both compounds **3** and **4** show only one reversible reduction wave, with  $E_{\text{red}}$  at -1.15 and -1.15 V, respectively. The first reduction potentials of **3** and **4** are much less negative than those of **1** and **2**,<sup>8</sup>

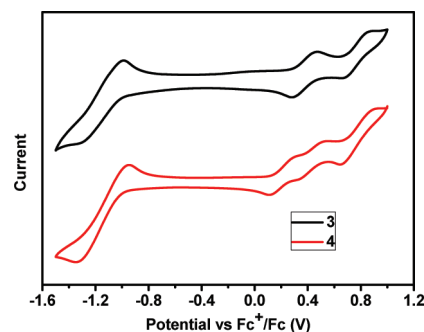


**FIGURE 4.** Cyclic voltammograms of compounds **3** and **4** in DCM with 0.1 M Bu<sub>4</sub>NPF<sub>6</sub> as supporting electrolyte, AgCl/Ag as reference electrode, Au disk as working electrode, Pt wire as counter electrode, and scan rate of 20 mV/s. Fc<sup>+</sup>/Fc was used as external reference.

revealing the extremely strong electron-accepting ability of **3** and **4** because of the imide group. Chemical oxidation titrations of compounds **3** and **4** were conducted in DCM by using SbCl<sub>5</sub> as an oxidant, and the process was followed by UV-vis-NIR absorption spectroscopy (Figure S9 in Supporting Information). Both compounds can be oxidized by SbCl<sub>5</sub> into stable radical cations with the appearance of new characteristic absorption bands in the shorter and longer wavelengths around the original NIR absorption band. The oxidized species can also be reversibly reduced into the neutral state upon adding Zn dust to the solution containing the oxidized species (Figure S10 in the Supporting Information). It is worth noting that upon exposure to sunlight, air-saturated solutions of **3** and **4** show no significant changes in their absorption spectra for months. Even under irradiation of a 4 W UV lamp (emitting at 254 nm) for 48 h, 95% of their initial optical density remains unchanged. The extraordinary stabilities of **3** and **4**, to our knowledge, are comparable to the most stable arylene compounds with NIR absorptions.<sup>15</sup> In contrast, the half-lives of **1** and **2** were estimated as 244 and 547 min, respectively, under the same UV irradiation conditions (Figure S11 in the Supporting Information) due to their relatively high-lying HOMO levels.

In summary, a facile one-pot synthesis of doubly and triply linked porphyrin–perylene monoimides **3** and **4** was established. It is worth noting that both *meta*- and *peri*-positions of perylene can be simultaneously involved in ring-closure reaction during the synthesis of the triply linked compound **4**. The introduction of an electron-withdrawing imide group effectively stabilizes the hybrid molecules. In addition, dyes **3** and **4**, with an intramolecular “push-pull” structure, display intensified NIR absorptions, large dipole moments, and high photostabilities, qualifying them as good NIR dyes for dye-sensitized solar cells. This requires further functionalization of the imide unit with anchoring groups, and the relevant work is underway in our laboratories.

## Experimental Section

**General Procedures.** All reagents were purchased from commercial suppliers and used as received without further purification. Anhydrous DCM and *N,N*-dimethylformaldehyde (DMF) were distilled from CaH<sub>2</sub>. Toluene and THF were distilled from

(14) Compound **3** emits very weak fluorescence in solution with a maximum at 828 nm, and the fluorescence quantum yield was less than 0.3% (Figure S2 in Supporting Information). For compound **4**, it is hard to determine any fluorescence under the same conditions. The low fluorescence quantum yields can account for the intramolecular charge transfer and the presence of Ni in the porphyrin units. The Ni-porphyrins usually have a low fluorescent quantum yield. For comparison, we also attempted to replace the Ni metal center with Zn. However, treatment of the dyes **3** and **4** with strong acid, such as CF<sub>3</sub>COOH or H<sub>2</sub>SO<sub>4</sub>, led to significant decomposition perhaps due to the relatively low HOMO energy levels of these compounds.

(15) (a) Geerts, Y.; Quante, H.; Platz, H.; Mahrt, R.; Hopmeier, M.; Böhm, A.; Müllen, K. *J. Mater. Chem.* **1998**, *8*, 2357–2369. (b) Pschirer, N. G.; Kohl, C.; Nolde, F.; Qu, J.; Müllen, K. *Angew. Chem., Int. Ed.* **2006**, *45*, 1401–1404.



sodium benzophenone immediately prior to use. The  $^1\text{H}$  NMR and  $^{13}\text{C}$  NMR spectra were recorded in  $\text{CDCl}_3$  or  $\text{C}_6\text{D}_6$  solution on NMR spectrometers with tetramethylsilane (TMS) as the internal standard. The chemical shift was recorded in ppm, and the following abbreviations were used to explain the multiplicities: s = singlet, d = doublet, t = triplet, m = multiplet, br = broad. Mass spectra were recorded with an EI ionization source. MALDI-TOF mass spectra were measured by using 1,8,9-trihydroxyanthracene as a matrix. Elemental analyses were performed only for C, H, and N elements. UV-vis absorption and fluorescence spectra were recorded in HPLC pure solvents. IR spectra were recorded by blending 1 wt % sample together with anhydrous KBr. The electrochemical measurements were carried out in anhydrous DCM with 0.1 M tetrabutylammonium hexafluorophosphate ( $\text{Bu}_4\text{NPF}_6$ ) as the supporting electrolyte at a scan rate of 0.02 V/s at room temperature under the protection of nitrogen. A gold disk was used as working electrode, platinum wire was used as counting electrode, and Ag/AgCl (3 M KCl solution) was used as reference electrode. The fluorescence quantum yields were measured by optical dilute method<sup>16</sup> ( $A < 0.05$ ) using Cardio-Green ( $\lambda_{\text{abs,max}} = 780 \text{ nm}$ ,  $\Phi = 0.13$  in DMSO) as reference.

**Compound 7.** Porphyrin **5** (91 mg, 1.1 equiv), **6** (61 mg, 1 equiv),  $\text{Pd}(\text{PPh}_3)_4$  (6 mg, 0.05 equiv), and  $\text{Cs}_2\text{CO}_3$  (65 mg, 2 equiv) were dried under vacuum and then purged with argon. To this were added degassed toluene (10 mL) and DMF (4 mL), and the mixture was stirred for 36 h at 96 °C. After cooling, water was added and the product was extracted with ethyl acetate ( $3 \times 10 \text{ mL}$ ). The organic layer was washed with saturated brine and dried over anhydrous  $\text{Na}_2\text{SO}_4$ . The solvent was removed under vacuum, and the residue was purified by column chromatography (silica gel, DCM/hexane, 1:1) to give a red, waxy solid product. Immediately, this solid was dissolved in toluene (10 mL), and  $\text{Ni}(\text{acac})_2$  (100 mg) was added slowly. The mixture was stirred for 40 h at 100 °C. After removal of the solvent, the crude product was purified by column chromatography (silica gel, hexane/DCM, 1:1) to give a red solid product, **7** (80 mg, 59% in two steps).  $^1\text{H}$  NMR ( $\text{CDCl}_3$ , 500 MHz)  $\delta$ : 9.32 (d,  $J = 5.1 \text{ Hz}$ , 2H), 9.26 (d,  $J = 4.4 \text{ Hz}$ , 2H), 8.88 (d,  $J = 5.1 \text{ Hz}$ , 2H), 8.83–8.86 (m, 2H), 8.76 (d,  $J = 7.6 \text{ Hz}$ , 2H), 8.61–8.63 (m, 2H), 8.57 (d,  $J = 8.2 \text{ Hz}$ , 1H), 8.46–8.47 (m, 2H), 7.78–7.91 (m, 3H), 7.53–7.56 (m, 1H), 7.40–7.43 (m, 2H), 7.17–7.22 (m, 1H), 7.07 (m, 1H), 4.76–4.82 (m, 2H), 4.39–4.46 (m, 2H), 2.86–2.91 (m, 2H), 2.15 (m, 2H), 0.71–1.60 (m, 62H).  $^{13}\text{C}$  NMR ( $\text{CDCl}_3$ , 125 MHz)  $\delta$ : 164.09, 164.07, 149.1, 145.8, 142.9, 142.6, 142.5, 141.6, 141.5, 141.45, 141.4, 139.7, 137.9, 137.7, 133.1, 132.3, 132.2, 132.0, 131.1, 130.9, 130.8, 130.7, 130.3, 130.2, 129.5, 129.4, 129.1, 128.8, 128.7, 127.6, 127.2, 127.0, 124.5, 124.0, 123.97, 123.7, 122.2, 121.3, 121.2, 120.6, 120.5, 119.1, 117.2, 114.1, 40.9, 39.4, 39.2, 39.1, 37.9, 37.8, 35.0, 33.8, 31.9, 31.7, 31.4, 30.2, 29.7, 27.9, 25.0, 24.1, 22.7, 22.6, 22.5, 20.0, 14.1. Anal. Calcd for  $\text{C}_{86}\text{H}_{93}\text{N}_5\text{NiO}_2$ : C, 80.23; H, 7.28; N, 5.44; Ni, 4.56; O, 2.49. Found: C, 80.04; H, 7.17; N, 5.51. (MALDI-TOF):  $m/z = 1286.567$  ( $\text{M} + \text{H}^+$ ); calcd for  $\text{C}_{86}\text{H}_{93}\text{N}_5\text{NiO}_2$ , 1285.668.

**Compound 3.** To a solution of **7** (40 mg, 1 equiv) in degassed anhydrous DCM (20 mL) was added a solution of  $\text{FeCl}_3$  (50 mg,

10 equiv) in nitromethane (0.5 mL). The reaction mixture was refluxed for 12 h and quenched by addition of a saturated  $\text{NaHCO}_3$  solution. The organic layer was washed with saturated brine and dried over anhydrous  $\text{Na}_2\text{SO}_4$ . The solvent was removed under vacuum, and the residue was purified by preparative TLC (DCM/hexane, 3:2) to give a purple solid product (15 mg, 38%).  $^1\text{H}$  NMR ( $\text{C}_6\text{D}_6$ , 500 MHz)  $\delta$ : 9.29 (s, 1H), 9.20 (d,  $J = 4.2 \text{ Hz}$ , 1H), 9.05 (d,  $J = 5.1 \text{ Hz}$ , 1H), 9.00 (d,  $J = 4.8 \text{ Hz}$ , 1H), 8.95 (d,  $J = 5.1 \text{ Hz}$ , 1H), 8.87–8.89 (m, 4H), 8.24 (br, 1H), 8.11 (br, 3H), 8.00–8.02 (m, 2H), 7.90 (m, 1H), 7.74 (br, 1H), 7.61–7.63 (m, 1H), 7.49–7.52 (m, 1H), 7.41–7.44 (m, 2H), 4.43–4.48 (m, 1H), 4.29 (m, 1H), 4.09–4.14 (m, 1H), 3.95 (m, 1H), 3.21–3.25 (m, 2H), 2.01–2.07 (m, 2H), 0.63–1.39 (m, 62H).  $^{13}\text{C}$  NMR ( $\text{CDCl}_3$ , 125 MHz)  $\delta$ : 164.04, 164.01, 149.5, 146.0, 144.1, 143.9, 142.8, 142.5, 141.6, 141.3, 140.3, 139.4, 138.5, 137.1, 136.9, 136.2, 133.9, 133.0, 132.6, 131.9, 131.8, 131.5, 130.7, 130.3, 129.5, 129.4, 128.4, 128.1, 126.3, 125.2, 124.4, 124.0, 123.9, 123.4, 121.5, 120.5, 120.0, 118.8, 40.8, 40.6, 39.2, 39.0, 38.8, 38.0, 37.8, 35.1, 31.7, 29.7, 29.3, 27.97, 27.95, 25.0, 24.1, 22.6, 22.4, 20.1. Anal. Calcd for  $\text{C}_{86}\text{H}_{91}\text{N}_5\text{NiO}_2$ : C, 80.36; H, 7.14; N, 5.45; Ni, 4.57; O, 2.49. Found: C, 80.59; H, 7.27; N, 5.69. (MALDI-TOF):  $m/z = 1284.231$  ( $\text{M} + \text{H}^+$ ); calcd for  $\text{C}_{86}\text{H}_{91}\text{N}_5\text{NiO}_2$ , 1283.653. IR (KBr):  $\nu = 2954, 2923, 2855, 1702, 1662, 1574, 1459, 1243, 1078, 1015, 791 \text{ cm}^{-1}$ .

**Compound 4.** Apart from the formation of **3** using the conditions mentioned above, **4** can be separated in 25% yield as a green solid.  $^1\text{H}$  NMR ( $\text{C}_6\text{D}_6$ , 500 MHz)  $\delta$ : 8.91 (d,  $J = 7.8 \text{ Hz}$ , 1H), 8.87 (d,  $J = 6.2 \text{ Hz}$ , 1H), 8.52 (br, 1H), 8.36–8.41 (br, 4H), 8.24 (br, 1H), 7.98 (br, 3H), 7.87 (br, 1H), 7.73 (br, 1H), 7.56 (br, 1H), 7.36–7.48 (m, 4H), 3.92 (br, 2H), 3.54 (br, 2H), 3.38 (br, 2H), 2.17–2.21 (m, 2H), 0.57–1.78 (m, 62H).  $^{13}\text{C}$  NMR ( $\text{C}_6\text{D}_6$ , 70 °C, 125 MHz)  $\delta$ : 164.4, 154.3, 153.3, 151.3, 147.6, 147.5, 147.1, 146.5, 145.4, 144.3, 143.3, 140.6, 136.8, 133.4, 133.3, 132.5, 127.5, 126.0, 124.4, 123.8, 123.4, 123.0, 121.7, 121.2, 118.6, 39.55, 39.49, 39.3, 35.8, 35.4, 31.5, 30.2, 30.0, 29.6, 28.4, 28.2, 25.6, 25.4, 24.6, 24.5, 23.0, 22.8, 22.7, 20.5, 20.0. Anal. Calcd for  $\text{C}_{86}\text{H}_{89}\text{N}_5\text{NiO}_2$ : C, 80.49; H, 6.99; N, 5.46; Ni, 4.57; O, 2.49. Found: C, 80.72; H, 7.15; N, 5.23. (MALDI-TOF):  $m/z = 1282.621$  ( $\text{M} + \text{H}^+$ ); calcd for  $\text{C}_{86}\text{H}_{89}\text{N}_5\text{NiO}_2$ , 1281.637. IR (KBr):  $\nu = 2958, 2925, 2854, 1697, 1627, 1461, 1357, 1261, 1094, 803 \text{ cm}^{-1}$ .

**Acknowledgment.** J.W. acknowledges the financial support from Singapore DSTA DIRP Project (DSTA-NUS-DIRP/2008/03), NRF Competitive Research Program (R-143-000-360-281), and NUS Young Investigator Award (R-143-000-356-101). K.-W.H. acknowledges the financial support from KAUST.

**Supporting Information Available:** Characterization data of all new compounds, absorption and emission spectra and data, electrochemical data, TDDFT calculation details, chemical oxidation titration experiments, and photostability test. This material is available free of charge via the Internet at <http://pubs.acs.org>.

(16) Licha, K.; Riefke, B.; Ntziachristos, V.; Becker, A.; Chance, B.; Semmler, W. *Photochem. Photobiol.* **2000**, *72*, 392–398.